JACS
JOURNAL OF THE AMERICAN CHEMICAL SOCIETY

Article

pubs.acs.org/JACS

Nonlinear Kinetic Behavior in Constitutional Dynamic Reaction Networks

Joseph J. Armao IV and Jean-Marie Lehn*

Laboratoire de Chimie Supramoléculaire, Institut de Science et d'Ingénierie Supramoléculaires (ISIS), Université de Strasbourg, 8 allée Gaspard Monge, 67000 Strasbourg, France

Supporting Information

ABSTRACT: Creating synthetic chemical systems which emulate the complexity observed in cells relies on exploiting chemical networks exhibiting nonlinear kinetic behavior. While control over reaction complexity using synthetic gene regulatory networks and DNA nanotechnology has developed greatly, little control exists over small molecule reaction networks. Toward this goal, we demonstrate a general framework for inducing nonlinear kinetic behavior in dynamic chemical networks based on molecules containing reversible chemical bonds. Specifically, this strategy relies on constituent species with differing thermodynamic stabilities that readily exchange components at rates that are faster than their formation rates. Such nonlinear networks (NLN) readily lead to sigmoidal kinetic profiles as a function of the relative thermodynamic stabilities of the constituent species. Furthermore, this behavior could be readily extended to more complex mixtures while maintaining nonlinearity. The generality of this method opens the possibility to generate nonlinear networks using a broad range of small molecule structures.

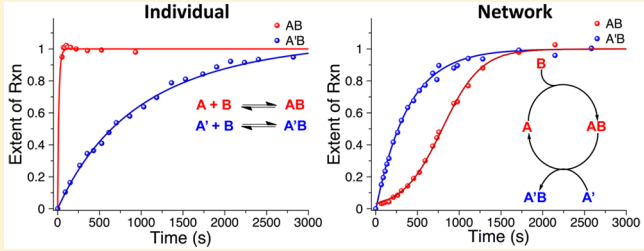

INTRODUCTION

Biochemical pathways consisting of interconnected reaction networks generate complexity and lead to the emergence of higher order functionality observed in living organisms. These networks exhibit nonlinear kinetic features allowing the temporal control over the appearance and disappearance of different molecular entities.[1−5] Current efforts toward emulating the complex kinetic behavior observed in cells make use of synthetic biology approaches involving in particular synthetic gene regulatory networks[6,7] or DNA nanotechnology implementing strand displacement reactions.[8−10] The control over small molecule network kinetic behavior is significantly less advanced.[11,12] One method for designing networks with complex behavior is to identify reactions displaying nonlinear kinetics, such as those exhibiting sigmoidal growth profiles, which would allow for temporal programming of molecular species in a network. For small organic molecules, such reactions are rather limited and comprise asymmetric amplification mechanisms with nonlinear effects[13] and autocatalytic mechanisms.[14,15] Among this small set of reactions, the majority either require a specific catalyst (asymmetric amplification reactions) or a strict structural design to induce the nonlinear behavior (autocatalytic behavior). Additionally, many of the reactions are irreversible, which prevents the incorporation into complex temporal profiles such as oscillations and feedback loops.

Here, we propose an alternative design methodology, which opens up a general method for achieving nonlinear kinetics and temporal control across a broad range of substrates. This methodology uses constitutional dynamic chemistry to create chemical networks based on species that may interconvert by virtue of reversible connections, either supramolecular interactions or covalent bonds formed via reversible reactions.[16,17]

Dynamic covalent chemistry (DCC) rests on the implementation of reversible chemical reactions[16] which may be linked together forming chemical reaction networks displaying adaptation behavior,[18] information storage,[19] and the ability to couple with nonequilibrium environments.[20] DCC systems based on C═N connections operate two different but linked processes: bond formation from a carbonyl component and an amino partner and component exchange. In this work, we elucidate the operation of a general acid-catalyzed process involving imine-type species that present different rates of formation and of interconversion as well as different thermodynamic stabilities. Acid catalysis induces rapid exchange between two species allowing for the formation of the thermodynamically more stable product first, followed by the sigmoidal growth of the less stable one, regardless of which species has the faster formation kinetics. More complex behaviors are demonstrated for networks displaying temporal separation, temporal cycling and linked kinetic evolution of constituents.

Received: October 25, 2016
Published: December 19, 2016

DOI: 10.1021/jacs.6b11107
J. Am. Chem. Soc. 2016, 138, 16809−16814

RESULTS AND DISCUSSION

Nonlinear network **NLN1** was generated from the dynamic covalent library (DCL)[16] of two amines (4-butylaniline **A** and 4-dimethylaminoaniline **A′**), an aldehyde (4-nitrobenzaldehyde **B**), and their respective imines (**AB** and **A′B**; Scheme 1). The

Scheme 1. Dynamic Covalent Library (DCL) Generating the Nonlinear Network NLN1

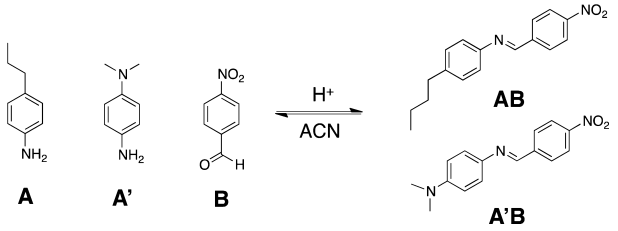

reaction kinetics upon mixing the amines and aldehydes were followed by NMR and examined both individually and the network arrangement of the DCL setup in acetonitrile under acid catalysis. The individual formation rates for each imine were determined to be 2.50 and 0.0529 M^{-1} s for **AB** and **A′B**, respectively (10 mM solutions of **A**, **A′**, and **B** each in acetonitrile with 10 mM DCl; Figure S1a,b), displaying a difference of nearly 2 orders of magnitude, as a result of the protonation of **A′**. Under the same conditions, the formation rates in the dynamic network setup of the DCL (Figures 1b, S2, and S3) lead to two striking changes in the kinetic profile: (1) The fastest accumulating imine switched from **AB** to **A′B**. (2) A sigmoidal growth profile was observed for imine **AB** formation. The graphical rate plots[21] (Figure S4) display the formation rates versus the concentrations of the component species. A linear dependence is observed with aldehyde **B** and amine **A′** while a nonlinear relationship is demonstrated with amine **A**. A sigmoidal function was used to fit the formation kinetics of imine **AB**:

$$f(x, n, m, t) = \frac{n}{1 + e^{-m(x-tx)}}$$

where the parameter n dictates the asymptotic height, or final imine concentration, m controls the slope, or maximal rate of imine formation, and t determines the onset delay, or lag time, of the sigmoidal function. The initial sigmoidal fit gave the values of n = 0.00571, m = 0.0043, and t = 796.89. Changing the starting concentrations while holding the relative acid content stable lead to a change in the sigmoidal response as displayed in Figure 1c (8, 10, 12 mM; Figures 1c and S5). The individual parameters, when plotted as a function of concentration (Figure S6), demonstrate a linear increase in the slope (m) and height (n) of the sigmoidal function as the concentration is increased. In contrast, the change in lag time (t) displayed a decrease with increasing concentration following a power law dependence.

Next, the acid content was varied while the starting concentrations were held constant at 10 mM. Drastic variations in the sigmoidal function resulted from increasing the acid content from 2.5 to 5, 7.5, 10, and 15 mM DCl (Figure 1d). At 15 mM DCl, the kinetics were fast enough that no appreciable time lag could be observed. Successful sigmoidal fits were performed for the rest of the tested conditions. The individual parameters demonstrated a linear increase in the height (n), an exponential increase in the slope (m), and an exponential decrease in the lag time (t) (Figure S7). Changing the acid content has a larger effect than changing the concentration on the slope, m, or reaction rate, as exhibited by the exponential relationships. Importantly, these results highlight the facility with which the sigmoidal function may be controlled by altering the concentrations of the starting species and the amount of acid present.

Kinetic analysis supports a nonlinear mechanistic interpretation of the observed behavior for several reasons. First, the formation of imine **A′B** occurs at a faster rate in the network configuration than is observed under identical conditions in the

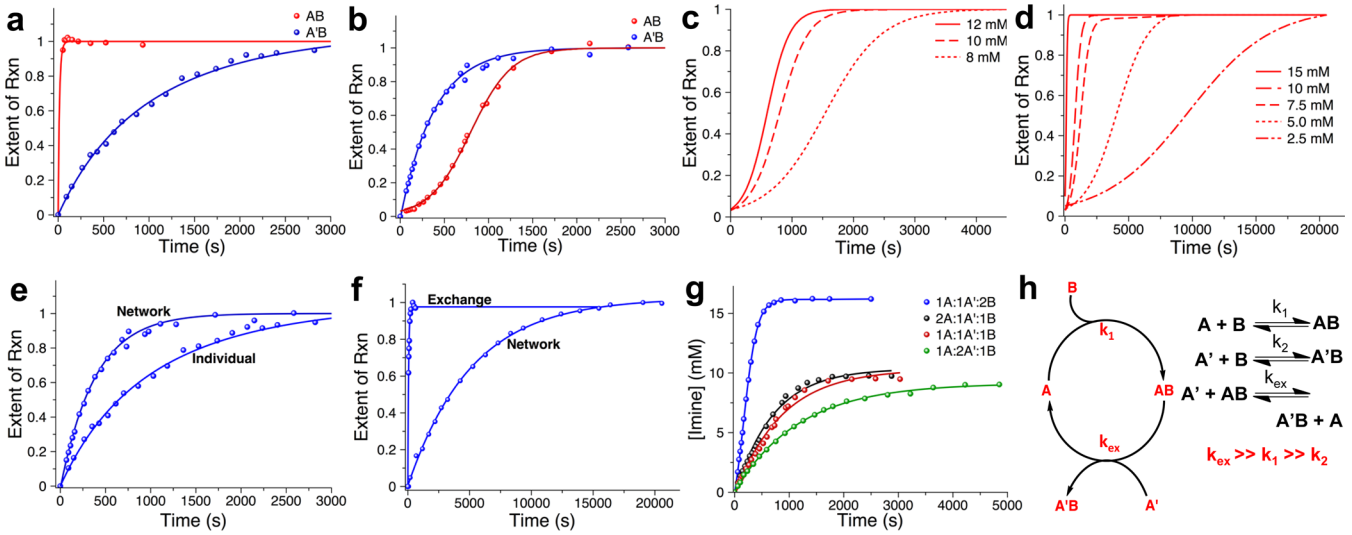

Figure 1. (a) Individual formation rates for **AB** and **A′B** (10 mM each) under acidic conditions (10 mM DCl) in acetonitrile. (b) Formation rates of **AB** and **A′B** in the network **NLN1** of a mixture of **A**, **A′**, and **B** under the same conditions as in (a), leading to a sigmoidal rate profile in **AB**. (c) Altering the concentration of the species or (d) the amount of acid (**A** and **A′** kept at 10 mM) in solution leads to a control over the sigmoidal rate profile for the formation of imine **AB**. (e) Comparative formation rate of **A′B** in the isolated and network **NLN1** case. (f) Comparative rates of formation (in the network) and exchange (separately determined). (g) Comparative overall imine formation rates at different stoichiometries. (h) Network formation cycle based on the kinetics parameters observed for the reactions on the left.

DOI: 10.1021/jacs.6b11107
J. Am. Chem. Soc. 2016, 138, 16809−16814

individual case (Figure 1e). Since these rates were observed under identical concentrations of reactants and acid, the direct formation from **A′** and **B** cannot explain this increase in the formation rate of imine **A′B** indicating that amine **A** must participate in the mechanism of **A′B** formation and play a catalytic role (see below).[22] Second, an overlay of the network formation rate **A′B** and the independently determined exchange rate of **A′** with imine **AB** (Figure 1f, 10 mM each species, 2.5 mM DCl) demonstrated that the exchange process occurs at a rate of 1.18 M^{-1} s, almost 2 orders of magnitude faster than the imine formation rate of 0.0211 M^{-1} s under identical conditions (Figure S9). This is a direct result of acid catalysis, which is known to promote rapid imine exchange rates that may otherwise proceed sluggishly in neutral conditions.[23] Third, by monitoring the total imine formation kinetics (Figure 1g), a linear combination of the formation of **AB** and **A′B**, one does not observe a clear switch in the rate at any point. Otherwise, two regimes should be apparent, one for the formation of **AB** and the other for the formation of **A′B**. Importantly, this means that as the rate of formation of **A′B** begins to plateau, the rate of formation of **AB** increases at an equivalent rate indicating a link in the mechanism between the appearances of the two species. This was consistently observed even with differing stoichiometric ratios of the component amines and aldehydes. Additionally, an experiment under the same conditions but containing 10 mM D_2O demonstrated only a slight retardation of the network formation rate, but showed no influence on the nonlinear behavior of the network (Figure S9). This rules out the in situ formation of water, produced during the course of imine formation, as the cause of the sigmoidal behavior.

The proposed cyclic mechanism describing network **NLN1** is depicted in Figure 1h and explains the observed nonlinear kinetic behavior. Imine **AB** has the fastest formation kinetics and therefore forms first in solution. However, under acid catalysis (involving imine activation by protonation) the imine exchange reaction between **AB** and **A′** proceeds rapidly allowing for the formation of **A′B** and the subsequent release of **A** from the intermediate aminal **AA′B**. The driving force for the accumulation of **A′B** over **AB** is due to the increased thermodynamic stability of the push–pull imine **A′B** in comparison with imine **AB**. As the production of **A′B** begins to slow, **AB** is allowed to accumulate leading to the sigmoidal kinetics.

The generality of this mechanism was demonstrated by examining networks based on a DCL of constituents containing reversible C═N bonds of three types with different thermodynamic stabilities: hydrazone, acylhydrazone and imine in order of decreasing stability (Scheme 2).[24] **NLN2** was constructed from three components, 4-butylaniline (**A**), benzhydrazide (**H**), and 4-butylbenzaldehyde (**B**) giving the hydrazone **HB** and imine **AB**. In contrast with **NLN1**, the formation rates for **HB** and **AB** were similar (Figure S10).

Scheme 2. Relative Thermodynamic Stabilities of the Three Reversible C═N Linkages: Hydrazone H′B, Acylhydrazone HB, and Imine AB

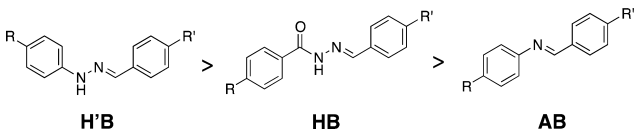

Kinetic experiments with a 1:1:1 mixture of **H**/**A**/**B** (8 mM each with 10% DCl in acetonitrile) displayed the formation of only acylhydrazone **HB** (Figure 2a). This confirms that **HB** is

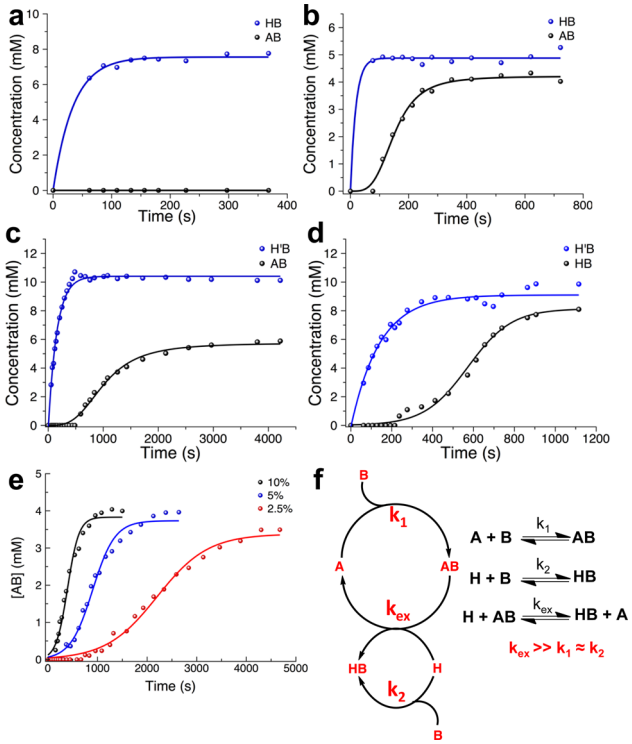

Figure 2. Behavior of different nonlinear networks of increasing complexity. (a) Formation kinetics of **NLN2** at 1:1:1 (8 mM, 10% DCl) and (b) at 1:1:2 (**H**/**A**/**B**; 5 mM, 10% DCl) stoichiometric ratios. Similar kinetic profiles were also observed for the networks (c) **NLN3** implementing 1:1:2 **H′**/**A**/**B** (10 mM, 5% DCl) as well as (d) **NLN4** with 1:1:2 **H′**/**H**/**B** (10 mM, 5% DCl). (e) Control over the sigmoidal profile of **NLN2** (1:1:2 case b) by altering the acid content from 10 to 2.5%. (f) Network **NLN2** formation cycles based on the kinetics parameters observed for the reactions on the right.

more stable than **AB**, while the suppression of the less stable imine **AB** highlights the presence of very fast exchange processes because the formation rates are similar. When the stoichiometry was changed to 1:1:2 **H**/**A**/**B**, we observed the formation of **HB** as well as the sigmoidal growth of imine **AB** (Figure 2b). The same nonlinear behavior was observed for **NLN3**, consisting of **H′B** and **AB** (using phenylhydrazine, **H′**; Figure 2c) as well as **NLN4**, consisting of **H′B** and **HB** (Figure 2d). In each case, the thermodynamically more stable species is formed first, followed by the less stable one. As with **NLN1**, by changing the amount of acid in solution, the sigmoidal profile could be altered (**NLN2**, Figure 2e and S11). The processes implemented in the generation of **NLN2** follow the kinetic cycles displayed in Figure 2f which emphasize that the formation of **HB** is due to both direct formation from **H** and **B** as well as exchange between **AB** and **H**. This behavior highlights that the generality of designing nonlinear networks necessitates (1) the formation of reversible chemical species with nonequivalent thermodynamic stabilities undergoing (2) rapid exchange between the two species at rates much larger than the formation rates, thereby allowing the formation of the thermodynamic product first, followed by the less stable one. Furthermore, there is no need for a fast and slow forming imine as perhaps seemed apparent from **NLN1**. The ability to

DOI: 10.1021/jacs.6b11107
J. Am. Chem. Soc. 2016, 138, 16809–16814

undergo rapid imine exchange (here due to acid catalysis) is the decisive factor.

Starting with these basic nonlinear networks, additional complexity may be built into the system. Here, we demonstrate three methods to achieve higher order complexity. First, the temporal separation of all three of the species depicted in Scheme 2 is realized. Using a four-component DCL consisting of 10 mM **A**, 10 mM **H**, 10 mM **H′**, and 30 mM **B** (0.5 mM DCl) leads to the sequential appearance of the three species in order of thermodynamic stability (Figure 3a, **NLN5**): The

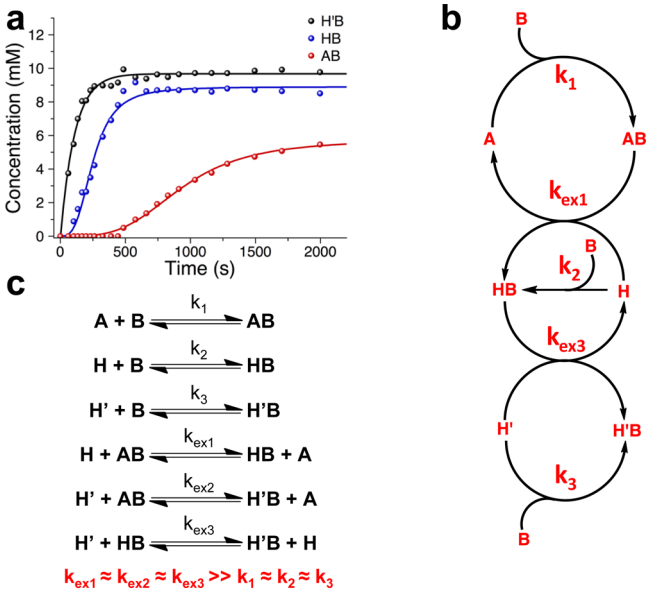

Figure 3. Behavior of the four-component (**H**, **H′**, **A**, **B**; 1:1:1:3) nonlinear network **NLN5**. (a) Kinetic profile demonstrating the temporal control through the nonlinear mechanism over the appearance of the species **H′B**, then **HB**, and finally **AB**. (b) Mechanistic cycles demonstrating the interconnected reactions (shown on the right) in the network (exchange 2 left out for visual clarity) leading to the nonlinear response.

initial growth of **H′B** is followed by the sigmoidal growth of **HB** and then the sigmoidal growth of **AB**. The corresponding mechanistic interconnected reaction cycles (Figure 3b) consist of a set of six reversible reactions: three formation reactions leading to **AB**, **HB**, and **H′B** and three exchange reactions between **AB**/**HB**, **AB**/**H′B**, and **HB**/**H′B**. On the basis of the above results, the observed behavior may be explained by the faster exchange kinetics as compared to the individual formation kinetics so that the order of appearance corresponds to the thermodynamic stabilities of the three species.

Second, temporal cycling of the nonlinear networks is achieved by altering the stoichiometry in time (Figure 4). Starting with **NLN2** in a 1:1:2 **H**/**A**/**B** stoichiometry (5 mM **H**/5 mM **A**/10 mM **B**; 0.25 mM DCl) gave the familiar profile observed above. The addition of a second equivalent of **H** at 2233 s leads to the rapid suppression of **AB** and a concomitant increase in species **HB** (Figure 4a). Taking this process one step further, starting with a 1:1:3 **H**/**A**/**B** solution (5 mM **H**/5 mM **A**/15 mM **B**; 0.25 mM DCl), once again one observes the familiar nonlinear profile, however, upon the addition of one equivalent of **H** at 3023 s the suppression of **AB** is followed by the subsequent sigmoidal recovery of **AB** (Figure 4b). Importantly, this course is due to the faster exchange reaction between **H** and **AB** as compared to the direct reaction of **H**

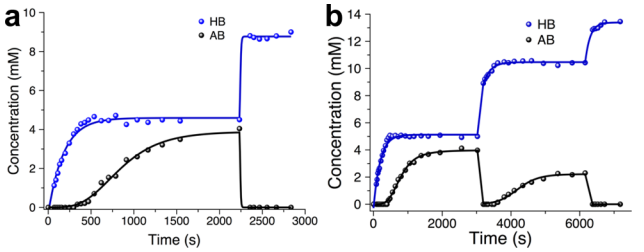

Figure 4. Temporal control over the reaction kinetics of the three component (**H**, **A**, **B**) network **NLN2** upon component addition. (a) Addition of one equivalent of **H** to a **NLN2** 1:1:2 (**H**/**A**/**B**) mixture and (b) two sequential additions of one equivalent of **H** to a 1:1:3 (**H**/**A**/**B**) mixture.

with free **B**. The thus newly liberated **A** then reacts with free **B** reforming **AB** with sigmoidal kinetics. Addition of a further equivalent of **H** at 6158 s leads to complete suppression of **AB**. These results clearly demonstrate the ability to restart the kinetic cycle in Figure 2f through the subsequent addition of **H** in the presence of excess **B**. The observed behavior highlights the importance of constructing networks through reversible bonds, which can easily continue to react with nonlinear behavior without being confined to a thermodynamic sink. This temporal control over the appearance of chemical species is an important first step toward building complex reaction circuits.

Third, linked kinetic evolution is realized by implementing a four-imine nonlinear network (**NLN6**) based on the DCL obtained by addition of 4-butylbenzaldehyde **B′** to the DCL of network **NLN1** (10 mM each species with 1 equiv, 10 mM, acid). The kinetic rate profiles display dual sigmoidal shape for the formation of imines **AB** and **AB′** (Figure 5a,b)

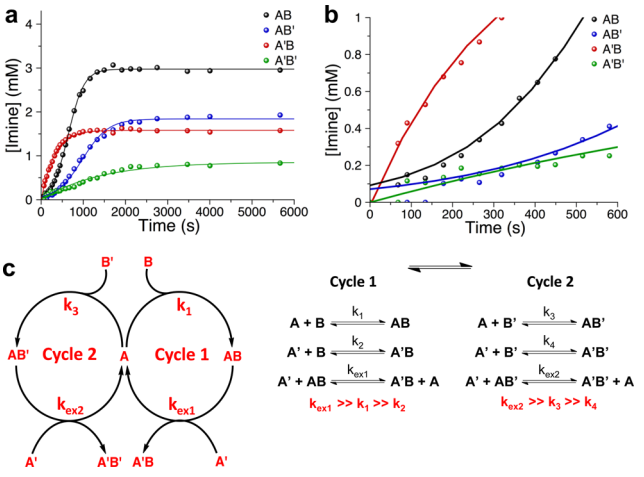

Figure 5. (a) Kinetic profiles for the formation of four constituents **AB**, **AB′**, **A′B**, and **A′B′** within the network **NLN6** with 10 mM starting concentrations of each species with 10 mM DCl displaying dual nonlinear shapes for the generation of **AB** and **AB′**. (b) Magnification of the initial 600 s of network formation. (c) Network graph representing the linked kinetic evolution of the formation of the four dynamic constituents involving component **A** as mechanistic hub.

demonstrating the possibility of creating parallel nonlinear kinetic networks. The network graph is shown in Figure 5c and displays two cycles connected through amine **A**, where cycle 1 is the same as **NLN1** described above and cycle 2 is constructed through the formation and exchange of imines **AB′** and **A′B′**. From the figure, it is clear that cycle 1 initiates the process, due

DOI: 10.1021/jacs.6b11107
J. Am. Chem. Soc. 2016, 138, 16809−16814

to the faster reacting aldehyde **B** (4-nitrobenzaldehyde). As detailed above, imine **A′B** is formed first, followed by the sigmoidal accumulation of **AB**. Cycle 2 lags slightly behind cycle 1, yet nevertheless displays concurrent sigmoidal behavior, with the initial formation of the exchange product **A′B′** followed by the sigmoidal rise of species **AB′**. In both cycles, the acid-catalyzed imine exchange takes place with amine **A′** to give exchange products **A′B** and **A′B′** which are thermodynamically favored due to the electron-donating dimethylamino group. The initial rise of these two imines is followed by the sigmoidal accumulation of their respective agonist imines **AB′** and **AB**. The distributions of the four imines with respect to different time points highlights the kinetic complexity which is available with a rather simple chemical system. For example, after 68 s we observe 77% **A′B**/23% **AB** which shifts to 61% **A′B**/18% **AB**/12% **A′B′**/9% **AB′** after 178 s and finally to 22% **A′B**/41% **AB**/11% **A′B′**/26% **AB′** after 3468 s.

CONCLUSION

In conclusion, we have demonstrated the implementation of nonlinear kinetics into chemical reaction networks. Such behavior may be induced in DCC systems based on chemical bonds formed by reversible reactions presenting coupled steps, wherein the formation rates of the individual constituents are slower than the rates of component exchange between them and the constituents present different stabilities. It is thus even the case for such an apparently simple process as imine formation and exchange. It offers a general strategy that should be readily adaptable to not just constitutional variations of the members of the DCLs described here but also the wide toolbox of available dynamic covalent bonds as well as to supramolecular interactions. This work represents a step in the implementation of kinetic features in complex network behavior.[25] Beyond small molecules and a single dynamic link, multifunctional molecules open processes of higher complexity presenting features such as feedback or oscillatory behavior, operating through thermodynamically and kinetically complex molecular networks.[26,27]

ASSOCIATED CONTENT

Supporting Information

The Supporting Information is available free of charge on the ACS Publications website at DOI: 10.1021/jacs.6b11107.

Methods, least-squares fit data, NMR spectra, sigmoidal fits and parameters, and imine distribution/network formation data (PDF)

AUTHOR INFORMATION

Corresponding Author

*E-mail: lehn@unistra.fr.

ORCID

Jean-Marie Lehn: 0000-0001-8981-4593

Notes

The authors declare no competing financial interest.

ACKNOWLEDGMENTS

We thank the ERC Advanced grant "SUPRADAPT" for financial support. J.A. acknowledges Dr. Valentina Garavini for support during the project.

REFERENCES

(1) Ferrell, J. E., Jr.; Machleder, E. M. *Science* **1998**, *280*, 895−898.
(2) Heinrich, R.; Neel, B. G.; Rapoport, T. A. *Mol. Cell* **2002**, *9*, 957−970.
(3) Koshland, D. E.; Goldbeter, A.; Stock, J. B. *Science* **1982**, *217*, 220−225.
(4) Angeli, D.; Ferrell, J. E.; Sontag, E. D. *Proc. Natl. Acad. Sci. U. S. A.* **2004**, *101*, 1822−1827.
(5) Becskei, A.; Serrano, L. *Nature* **2000**, *405*, 590−593.
(6) Gardner, T. S.; Cantor, C. R.; Collins, J. J. *Nature* **2000**, *403*, 339−342.
(7) Endy, D. *Nature* **2005**, *438*, 449−453.
(8) Yurke, B.; Turberfield, A. J.; Mills, A. P., Jr.; Simmel, F. C.; Neumann, J. L. *Nature* **2000**, *406*, 605−608.
(9) Zhang, D. Y.; Winfree, E. *J. Am. Chem. Soc.* **2009**, *131*, 17303−17314.
(10) (a) Zhang, D. Y.; Seelig, G. *Nat. Chem.* **2011**, *3*, 103−113. (b) Soloveichik, D.; Seelig, G.; Winfree, E. *Proc. Natl. Acad. Sci. U. S. A.* **2010**, *107*, 5393−5398. (c) Montagne, K.; Plasson, R.; Sakai, Y.; Fujii, T.; Rondelez, Y. *Mol. Syst. Biol.* **2011**, *7*, 466. (d) Padirac, A.; Fujii, T.; Rondelez, Y. *Proc. Natl. Acad. Sci. U. S. A.* **2012**, *109*, E3212−E3220. (e) Chen, Y.-J.; Dalchau, N.; Srinivas, N.; Phillips, A.; Cardelli, L.; Soloveichik, D.; Seelig, G. *Nat. Nanotechnol.* **2013**, *8*, 755−762.
(11) Grzybowski, B. A.; Huck, W. T. S. *Nat. Nanotechnol.* **2016**, *11*, 585−592.
(12) Li, J.; Nowak, P.; Otto, S. *J. Am. Chem. Soc.* **2013**, *135*, 9222−9239.
(13) Girard, C.; Kagan, H. B. *Angew. Chem., Int. Ed.* **1998**, *37*, 2922−2959.
(14) Soai, K.; Shibata, T.; Morioka, H.; Choji, K. *Nature* **1995**, *378*, 767−768.
(15) Bissette, A. J.; Fletcher, S. P. *Angew. Chem., Int. Ed.* **2013**, *52*, 12800−12826.
(16) For a selection of reviews specifically on dynamic covalent chemistry, see for instance (a) Lehn, J.-M. *Chem. - Eur. J.* **1999**, *5*, 2455−2463. (b) Rowan, S. J.; Cantrill, S. J.; Cousins, G. R.; Sanders, J. K. M.; Stoddart, J. F. *Angew. Chem., Int. Ed.* **2002**, *41*, 898−952. (c) Corbett, P. T.; Leclaire, J.; Vial, L.; West, K. R.; Wietor, J.-L.; Sanders, J. K. M.; Otto, S. *Chem. Rev.* **2006**, *106*, 3652−3711. (d) Ladame, S. *Org. Biomol. Chem.* **2008**, *6*, 219−226. (e) Miller, B. L. *Dynamic Combinatorial Chemistry*; Wiley, Chichester, 2010. (f) Reek, J. N. H.; Otto, S. *Dynamic Combinatorial Chemistry*; Wiley-VCH, Weinheim, 2010. (g) Hunt, R. A. R.; Otto, S. *Chem. Commun.* **2011**, *47*, 847−855. (h) Belowich, M. E.; Stoddart, J. F. *Chem. Soc. Rev.* **2012**, *41*, 2003−2024.
(17) For constitutional dynamic networks, see (a) Lehn, J.-M. *Angew. Chem., Int. Ed.* **2013**, *52*, 2836−2850. (c) Lehn, J.-M. *Angew. Chem., Int. Ed.* **2015**, *54*, 3276−3289. (b) Lehn, J.-M.; Barboiu, M. *Top. Curr. Chem.* **2011**, *322*, 1−32.
(18) For recent examples of constitutional dynamic networks, see, for instance (a) Ulrich, S.; Lehn, J.-M. *Chem. - Eur. J.* **2009**, *15*, 5640−5645. (b) Lao, L.; Schmitt, J.-L.; Lehn, J.-M. *Chem. - Eur. J.* **2010**, *16*, 4903−4910. (c) Vantomme, G.; Jiang, S. M.; Lehn, J.-M. *J. Am. Chem. Soc.* **2014**, *136*, 9509−9518. (d) Hafezi, N.; Lehn, J.-M. *J. Am. Chem. Soc.* **2012**, *134*, 12861−12868. (e) Vantomme, G.; Hafezi, N.; Lehn, J.-M. *Chem. Sci.* **2014**, *5*, 1475−1483. (f) for chemical reaction networks, see for instance van Roekel, H. W. H.; Rosier, B. J. H. M.; Meijer, L. H. H.; Hilbers, P. A. J.; Markvoort, A. J.; Huck, W. T. S.; de Greef, T. F. A. *Chem. Soc. Rev.* **2015**, *44*, 7465−7483. (g) For interaction networks, see for example Ghosh, S.; Mukhopadhyay, M.; Isaacs, L. *J. Syst. Chem.*, **2010**, *1*, DOI: 10.1186/1759-2208-1-6.
(19) Holub, J.; Vantomme, G.; Lehn, J.-M. *J. Am. Chem. Soc.* **2016**, *138* (36), 11783−11791.
(20) Armao, J. J.; Lehn, J.-M. *Angew. Chem., Int. Ed.* **2016**, *55* (43), 13450−13454.
(21) Blackmond, D. G. *Angew. Chem., Int. Ed.* **2005**, *44*, 4302−4320.
(22) Cordes, E. H.; Jencks, W. P. *J. Am. Chem. Soc.* **1962**, *84* (5), 826−831.

DOI: 10.1021/jacs.6b11107
J. Am. Chem. Soc. 2016, 138, 16809−16814

(23) Giuseppone, N.; Schmitt, J.-L.; Schwartz, E.; Lehn, J.-M. *J. Am. Chem. Soc.* **2005**, *127*, 5528−5539.
(24) Kalia, J.; Raines, R. T. *Angew. Chem., Int. Ed.* **2008**, *47*, 7523−7526.
(25) (a) Nicolis, G.; Nicolis, C. *Foundations of Complex Systems*; World Scientific Pub. Co.: Singapore, 2012. (b) Hjelmfelt, A.; Weinberger, E. D.; Ross, J. *Proc. Natl. Acad. Sci. U. S. A.* **1991**, *88*, 10983−10987. (c) Hjelmfelt, A.; Schneider, F. W.; Ross, J. *Science* **1993**, *260*, 335.
(26) For complex networks, see for instance (a) Cohen, R.; Havlin, S. *Complex Networks*; Cambridge University Press: Cambridge, U.K., 2010. (b) Ref 25a. (c) Benson, A. R.; Gleich, D. F.; Leskovec, J. *Science* **2016**, *353*, 163−166.
(27) The present results may also play a role towards developing novel asymmetric catalysis reactions.

DOI: 10.1021/jacs.6b11107
J. Am. Chem. Soc. 2016, 138, 16809−16814